Electroluminescence from Singlet Excited-State of the Exciplex between (2,3-Dicarbonitrilopyrazino[2,3-f][1,10]phenanthroline)Re(CO)$_3$Cl and CBP

Zhenjun Si,[†,‡] Jiang Li,[§] Bin Li,*[,†] Ziruo Hong,[†] Shiyong Liu,*[,§] and Wenlian Li[†]

Key Laboratory of Excited State Processes, Changchun Institute of Optics, Fine Mechanics and Physics, and Graduate School of the Chinese Academy of Sciences, Chinese Academy of Sciences, Changchun 130033, P. R. China, and State Key Laboratory of Integrated Optoelectronics, Jilin University, Changchun 130023, P. R. China

Received: July 17, 2007; In Final Form: December 4, 2007

(2,3-Dicarbonitrilopyrazino[2,3-f] [1,10]phenanthroline)Re(CO)$_3$Cl (Dicnpp-Re) is synthesized successfully, and the photophysics, the electrochemistry, and the thermogravimetric analysis are performed to study the properties of Dicnpp-Re. It is found that the exciplex with λ_{max} at ~620 nm can be formed between CBP and Dicnpp-Re, and the exciplex emission is confirmed to be from the singlet excited state of the bound CBP and Dicnpp-Re molecules by the measurement of the lifetime of the CBP/Dicnpp-Re film. Color-tunable EL devices based on a host material of CBP and a dopant material of Dicnpp-Re are fabricated. A CBP/Dicnpp-Re (3%) based EL device emits white light with CIE coordinates of ($x = 0.35$, $y = 0.32$). The spectrum consists of three discrete bands centered at 380 nm from CBP, 560 nm from the characteristic ^{3}MLCT state of Dicnpp-Re, and 620 nm from the exciplex between Dicnpp-Re and CBP. When the doping concentration is 16%, the EL spectrum mainly demonstrates the red exciplex emission with CIE coordinates of ($x = 0.57$, $y = 0.33$).

1. Introduction

Since Forrest et al. reported that electrophosphorescent materials could harvest both singlet and triplet excitons and endowed organic light-emitting devices (OLEDs) with a potential internal quantum efficiency of 100%,[1] the electrophosphorescence of heavy metal complexes has been studied extensively.[2−4] OLEDs based on tricarbonyl diimine rhenium (Re) complexes[3−6] also attract much attention because of their advantages, such as excellent thermal stability, high room temperature (RT) phosphorescence quantum yield, and so forth. By now, electroluminescent (EL) performance of Re(I) complexes has been improved greatly owing to the molecular design and modification.[7]

An exciplex, originally short for excited complex, is a short-lived heterodimeric molecule formed from two species, at least one of which is in an electronic excited state. Unlike excitons within single molecule sites, during the exciplex formation the wavefunction of excited states extends over the molecules and the molecules are bound together only in the excited state and not in the ground state. Because of the longer excited-state lifetimes, the formation of an exciplex is usually unfavorable to improve EL efficiency.[8,9] However, the new emission band from the exciplexes is beneficial to realize color-tuning[8,10] and/or white OLEDs[9,11] and to improve the performance of the organic photovoltaic cells.[12] Up to date, the EL devices based on the exciplex emission from heavy metal complexes are seldom studied,[13−15] and there is no report for Re(I) complexes.

In this paper, we report the color-tunable EL devices with (2,3-dicarbonitrilopyrazino[2,3-f] [1,10]phenanthroline)Re(CO)$_3$Cl (Dicnpp-Re) being employed as a dopant in the (4,4′-*N*,*N*′-dicarbazole) biphenyl (CBP) layer. When the doping concentration of Dicnpp-Re is 3%, the white EL device, which exhibits violet emission from CBP and yellow from the complex, as well as red from exciplex between CBP and Dicnpp-Re, offers a maximum brightness of 1457 cd/m^2 and a peak efficiency of 1.6 cd/A.

2. Experimental Section

2.1. Measurement. *2.1.1. Spectroscopy.* The IR spectra were acquired using a Magna560 FT-IR spectrophotometer. Element analyses were performed using a Vario Element Analyzer. ^{1}H NMR spectra were obtained using a Bruker AVANVE 500 MHz spectrometer with tetramethylsilane as the internal standard. The absorption and photoluminescence spectra were recorded on a Shimadzu Model 3100 spectrometer and a Hitachi Spectrophotometer model F-4500, respectively. EL spectra and the Commission Internationale de L'Eclairage (CIE) coordinates of the devices were measured by a PR650 spectrometer under ambient conditions. The measurements of the excited-state lifetime were carried out on a FL920 single-photon spectrometer with a nanosecond flashlamp (pulse width, 1 ns; repetition rate, 40 kHz).

2.1.2. Crystallography. The crystals of Dicnpp-Re were measured on a Bruker Smart Apex CCD single-crystal diffractometer using λ (Mo KR) radiation, 0.7107 Å at 293 K. An empirical absorption was based on the symmetry-equivalent reflections and applied to the data using the SADABS program. The structure was solved using the SHELXL-97 program.[16] The crystallographic refinement parameters of Dicnpp-Re are summarized in Table 1, and the selected bond distances and angles are given in Table 2.

* Authors to whom correspondence should be addressed. E-mail: lib020@ciomp.ac.cn (B. Li); syliu@mail.jlu.edu.cn (S. Liu). Fax: +86 0431 86176935 (B. Li).
† Changchun Institute of Optics, Fine Mechanics and Physics.
‡ Graduate School of the Chinese Academy of Sciences.
§ Jilin University.

10.1021/jp075621u CCC: $40.75
Published on Web 02/16/2008

TABLE 1: Crystal Data and Structure Refinement for Dicnpp-Re

formula	$C_{19}H_6N_6O_3ReCl$
fw	587.95
T (K)	293(2)
wavelength (Å)	0.71073
cryst syst	orthorhombic
space group	Pnma
a (Å)	9.8410(6)
b (Å)	14.0813(8)
c (Å)	14.0276(8)
α (deg)	90
β (deg)	90
γ (deg)	90
V (Å^3)	1943.9(2)
Z	4
ρ_{calcd} (mg/m^3)	1.886
μ (mm^{-1})	6.416
F (000)	1040
crystal size	0.350 × 0.227 × 0.213 mm^3
range of transm factors (deg)	2.05−28.30
reflections collected	11367
unique	2423
completeness to $\theta = 28.30$	96.30%
data/restraints/parameters	2423/0/142
GOF on F^2	1.014
$R1$, w$R2$ [$I > 2\sigma(I)$]	0.0258, 0.0511
$R1$, w$R2$ (all data)	0.0436, 0.0563

TABLE 2: Bond Lengths (Å) and Angles (deg) for Dicnpp-Re

C(1)−O(1)	1.151(5)	C(8)−N(2)	1.356(4)
C(1)−Re(1)	1.913(5)	C(9)−N(2)	1.326(5)
C(2)−O(2)	1.157(6)	N(1)−Re(1)	2.172(3)
C(2)−Re(1)	1.889(7)	Cl(1)−Re(1)	2.4959(15)
C(3)−N(1)	1.362(4)	Re(1)−C(1A)	1.913(5)
C(4)−N(1)	1.339(4)	Re(1)−N(1A)	2.172(3)
O(1)−C(1)−Re(1)	178.9(4)	C(1)−Re(1)−N(1A)	171.78(13)
O(2)−C(2)−Re(1)	177.8(5)	C(1A)−Re(1)−N(1A)	97.62(14)
N(1)−C(3)−C(7)	122.9(3)	C(2)−Re(1)−N(1)	94.67(15)
N(1)−C(3)−C(3A)	116.13(18)	C(1)−Re(1)−N(1)	97.62(14)
N(1)−C(4)−C(5)	122.9(4)	C(1A)−Re(1)−N(1)	171.78(13)
C(4)−N(1)−Re(1)	127.7(3)	N(1A)−Re(1)−N(1)	75.15(15)
C(3)−N(1)−Re(1)	114.9(2)	C(2)−Re(1)−Cl(1)	177.40(17)
C(2)−Re(1)−C(1)	89.77(18)	C(1)−Re(1)−Cl(1)	92.08(13)
C(2)−Re(1)−C(1A)	89.77(18)	C(1A)−Re(1)−Cl(1)	92.08(13)
C(1)−Re(1)−C(1A)	89.3(2)	N(1A)−Re(1)−Cl(1)	83.28(8)
C(2)−Re(1)−N(1A)	94.67(15)	N(1)−Re(1)−Cl(1)	83.28(8)

2.1.3. Thermal Analysis. Thermogravimetric analysis (TGA) was performed on ∼2 mg of Dicnpp-Re using a Perkin-Elmer Thermal analyzer. The samples were dried under vacuum at 56.5 °C before being heated from 50 to 500 °C at a heating rate of 10.0 °C/min. A 10 mL/min flow of dry nitrogen was used to purge the sample during the whole process.

2.1.4. Cyclic Voltammetry. Cyclic voltammetry measurements were conducted on a voltammetric analyzer (CH Instruments, Model 620B) with a polished Pt plate as the working electrode, Pt mesh as the counter electrode, and a commercially available saturated calomel electrode (SCE) as the reference electrode, at a scan rate of 0.1 V/s. The voltammograms were recorded using CH_3CN sample solutions with $\sim10^{-3}$ M Dicnpp-Re and 0.1 M ammonium hexafluorophosphate (AHFP) as the supporting electrolyte. Prior to each electrochemical measurement, the solution was purged with nitrogen for ∼10−15 min to remove the dissolved O_2 gas. and the energy level of highest occupied molecular orbital (E_{HOMO}) was calculated according to ref 17.

2.1.5. Atomic Force Microscopy (AFM) Images. AFM images of pure CBP and 10% Dicnpp-Re doped CBP films were obtained in normal air conditions at RT by a commercial atomic force microscope (Di3100s, Veeco) with a scan size of 25 μm^2. The data scales are 120 and 20 nm for pure CBP and 10% Dicnpp-Re-doped CBP films, respectively. The sample films were deposited on previously cleaned indium tin oxide (ITO) substrates by thermal deposition and then kept 24 h in a glovebox under N_2 atmosphere.

2.2. Materials. All of the starting chemicals and charge-transporting materials used in the process of the EL device's fabrication, 4,4′,4″-tris[3-methylphenylphenylamino]triphenylamine (*m*-MTDATA), 4,7-diphenyl-1,10-phenanthroline (Bphen), 4,4′-bis[*N*-(1-naphthyl)-*N*-phenylamino]biphenyl (NPB), CBP, tris(8-hydroxy-quinoline)aluminum (Alq_3), and LiF, were commercially available and used without further purification unless otherwise noted. The ligand Dicnpp[18] and the corresponding Re(I) complex, Dicnpp-Re,[19] are synthesized according to the reported methods. The synthesis route of Dicnpp-Re is depicted in Scheme 1. All reactions and manipulations were carried out under N_2 with the use of standard inert atmosphere and Schlenk techniques. The solvents used for synthesis were dried by standard procedures and stored under N_2. The solvents used in the luminescent and electrochemical studies were of spectroscopic and anhydrous grades, respectively.

2.2.1. Synthesis of Dicnpp. A fine powder mixture of 2.000 g of 1,10-phenanthroline and 3.000 g of KBr was added into an ice-cooled flask containing 20 mL of H_2SO_4 (98%). After the mixture was cooled sufficiently, 10 mL of dense HNO_3 was added dropwise. After heating at 40 °C for 6 h, the reaction system was heated at 80 °C for another 2 h, and then the produced liquid Br_2 was pumped out the flask. The residue cool mixture was poured into ice water, and NaOH aqueous solution was added to make the pH of the solution ∼6−7 and then was extracted by chloroform. After dryinh by Na_2SO_4, chloroform was removed by rotation evaporation. The residue was recrys-

SCHEME 1

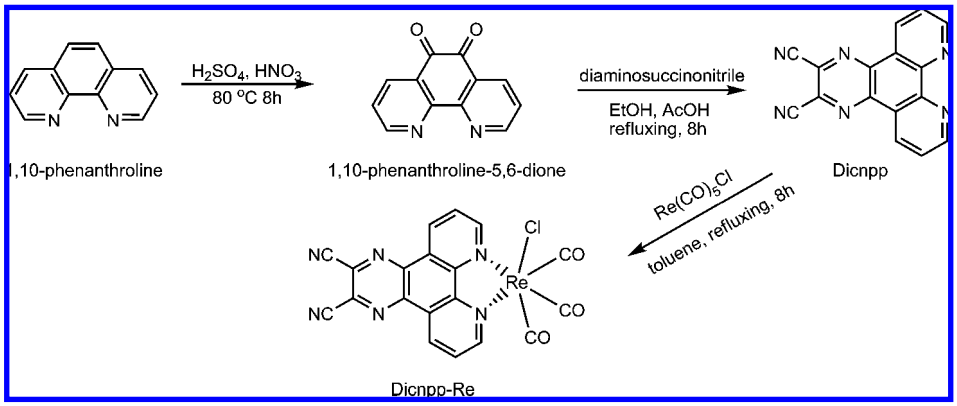

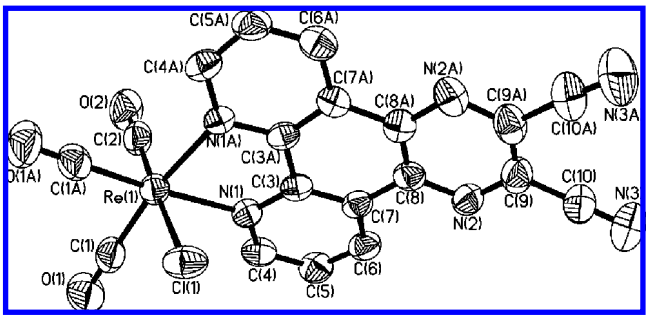

Figure 1. ORTEP drawing of a crystal of Dicnpp-Re with displacement ellipsoids at the 50% probability level.

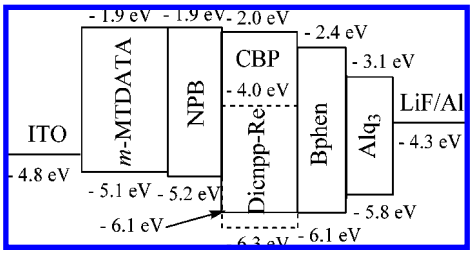

Figure 2. Energy diagram of EL devices.

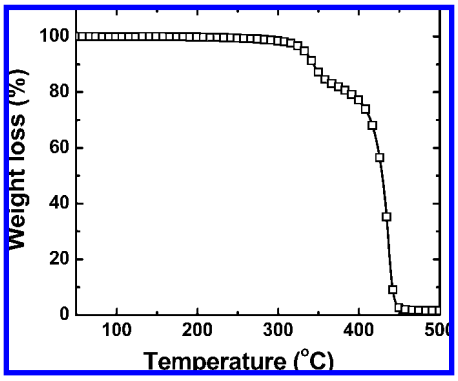

Figure 3. TGA traces for Dicnpp-Re complexes.

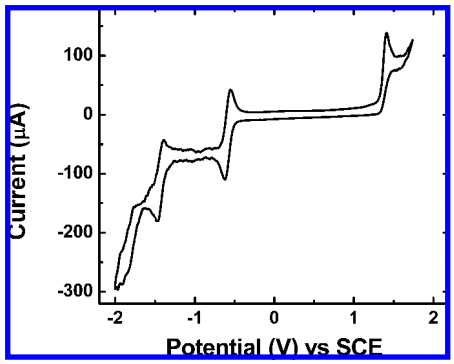

Figure 4. Cyclic voltammograms of complexes **1** and **2** measured in CH_3CN (vs SCE) at a scan rate of 0.1 V/s. A polished Pt plate and a Pt mesh were used as the working electrode and the counter electrode, respectively. AHFP was taken as the supporting electrolyte.

tallized from methanol to yield yellow 1,10-phenanthroline-5,6-dione. A mixture of 1.050 g of 1,10-phenanthroline-5,6-dione and 0.650 g of diaminomaleonitrile, together with a few drops of acetic acid, was added into 50 mL of ethanol in a flask, and the solution was stirred and refluxed under the protection of the N_2 gas. After the reaction was finished, the solution was cooled to RT and poured into 100 mL of H_2O; then the solid was filtered and recrystallized from methanol to yield brown powder Dicnpp. Yield: 91%. ^{1}H NMR ($CDCl_3$): 9.357 (d, 2H, J = 8), 9.324 (d, 2H, J = 3), 8.006 (m 2H, J = 4). IR (KBr)/cm^{-1}: 3400, 3069, 2240, 1585, 1461. Anal. Calcd. for $C_{16}H_6N_6$: C, 68.08; H, 2.14; N, 29.77. Found: C, 67.99; H, 2.19; N, 29.53. UV−vis: 267 nm, 308 nm, 370 nm.

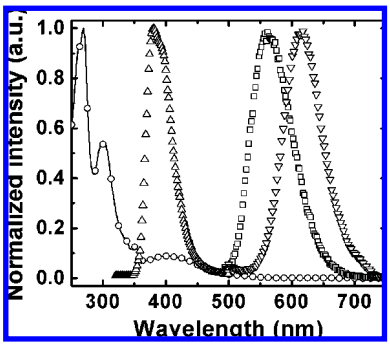

Figure 5. Absorption spectrum of Dicnpp-Re in dilute dichloromethane (open circle and line) and the PL spectra of Dicnpp-Re (open square), CBP (open triangle), and CBP/Dicnpp-Re (50%) films (open reverse triangle).

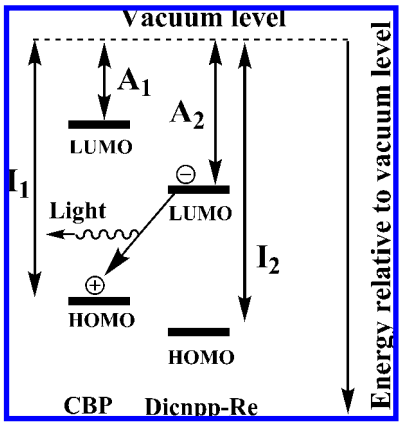

Figure 6. Energy level diagram showing the mechanism of exciplex formation. A_1, I_1 and A_2, I_2 are the electron affinities and ionization potentials of CBP and Dicnpp-Re, respectively.

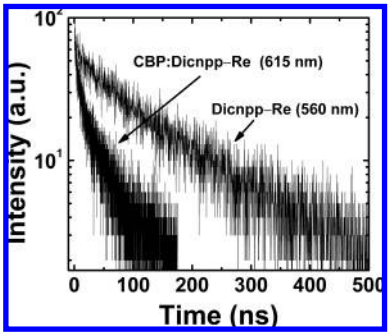

Figure 7. Excited-stated decay lifetimes of the Dicnpp-Re and CBP/Dicnpp-Re (50%) films.

2.2.2. Synthesis of Dicnpp-Re. The mixture of Dicnpp (0.06 g) and $Re(CO)_5Cl$ (0.07 g) was refluxed in 15 mL of toluene for 6 h. After cooling to RT, the solvent was removed in a water bath under reduced pressure. The resulting yellow solid was purified by silica gel column chromatography with acetic acid ethyl ester and dichloromethane (v/v = 10: 1). Yield: 0.10 g (~80%). ^{1}H NMR ($CDCl_3$): 9.675 (d, 2H, J = 8.8), 9.613 (d, 2H, J = 4.5), 8.149 (m 2H, J = 5). IR (KBr)/cm^{-1}: 2024, 1924, 1875. Anal. Calcd. for $C_{19}H_6ClN_6O_3Re$: C, 38.81; H, 1.03; N, 14.29. Found: C, 38.79; H, 1.10; N, 14.33. UV−vis: 270 nm, 303 nm, 352 nm, 402 nm.

2.3. Fabrication of the OLEDs. As can be seen from Figure 2, the general structure of the EL devices based on Dicnpp-Re

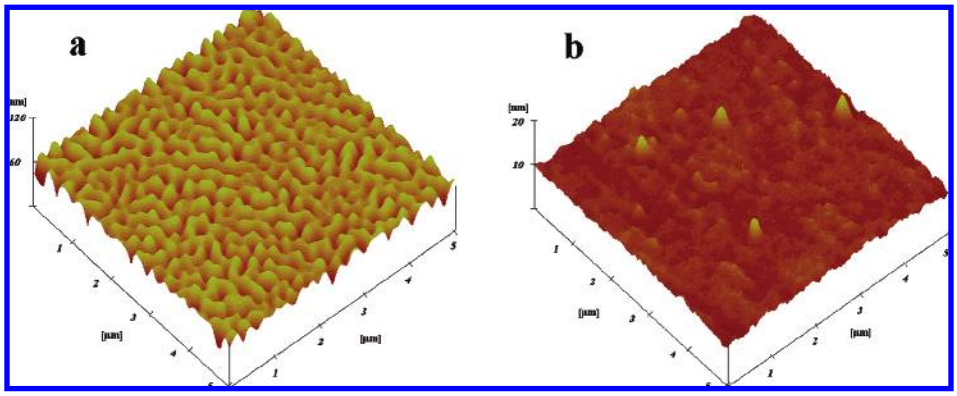

Figure 8. AFM images of the films of the pure CBP (a) and 10% Dicnpp-Re doped CBP (b).

is as follows: ITO/*m*-MTDATA (30 nm)/NPB (20 nm)/CBP/Dicnpp-Re (*x* wt %, 30 nm) Bphen (20 nm)/Alq_3 (20 nm)/LiF (0.8 nm)/Al (200 nm), where *m*-MTDATA, NPB, Bphen, and Alq_3 were used as the hole-injection layer, the hole-transporting layer, the electron-transporting layer, and the electron-injection layer, respectively. CBP doped with Dicnpp-Re acted as the luminescent layer. All layers of the devices were deposited on ITO substrates by thermal deposition at a pressure of 3×10^{-4} Pa. The shadow masks were used to define the electrode areas of 4 mm^2.

3. Results and Discussion

Synthesis and Characterization. Ligand Dicnpp and the corresponding Re(I) complex Dicnpp-Re were prepared according to the literature methods, and their structures are shown in Scheme 1. The purity and composition of the complexes were confirmed by ^1H NMR, IR, and elemental analyses. The ^1H NMR spectrum of Dicnpp-Re has some differences from those of the corresponding free diimine ligand Dicnpp. Compared to the free ligand, these signals were shifted toward low field because of the formation of new coordination bonds between the synthesized ligand and the Re metal centers.[20]

Structure of Dicnpp-Re. Using the single-crystal X-ray diffraction method, we obtained solid evidence to support the structure of Dicnpp-Re. An ORTEP diagram of Dicnpp-Re is shown in Figure 1, and the crystal data are presented in Table 1; selected bond distances and angles for the complexes are listed in Table 2. The coordination geometry at the Re atom is a distorted octahedron with the three carbonyl ligands arranged in a facial fashion. The distances of C(1), C(1A), and C(2) to Re(1) are 1.913(5), 1.913(5), and 1.889(7) Å, respectively, and both distances of Re(1)−N(1) and Re(1)−N(1A) bond are 2.172 (3) Å, indicating that the molecules of Dicnpp-Re have bilateral symmetry, which is also proven by the angle data presented in Table 2: The CO ligands are linearly coordinated, and the angles of C(1)−Re(1)−C(1A), C(1)−Re(1)−C(2), and C(1A)−Re(1)−C(2) are 89.3(2)°, 89.77(18), and 89.77(18), respectively. The angle of N(1)−Re−N(1A) is only 75.15(15)°, which should be attributed to the steric requirement of the bidentate coordination of Dicnpp. All other bond distances and angles are comparable to those found for the related Re(I) complexes.[21]

Thermal Analysis. TGA was performed on Dicnpp-Re in N_2 atmosphere to investigate its stable characteristics, and the TGA trace of Dicnpp-Re is presented in Figure 3. Dicnpp-Re began to lose weight when it was heated up to 325 °C, which should be attributed to the loss of the chloride anion and carbonyl groups. Dicnpp probably began to dramatically disassociate or sublimate at 410 °C and totally decomposed at

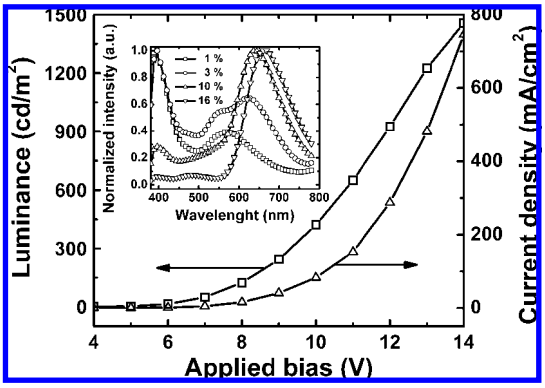

Figure 9. *J*−*L*−*V* characteristics of 3% doped devices. Inset: EL spectra of the EL devices based on different doping concentrations at 13 V.

450 °C. Therefore, Dicnpp-Re should be stable enough to be sublimated to construct OLED devices at ∼300 °C.

Electrochemistry. Cyclic voltammograms of Dicnpp-Re are shown in Figure 4 and exhibit irreversible metal-centered oxidation, which is consistent with the redox behavior of Pybm-based Re(I) diimine complexes reported in the literature[5] and reversible ligand-based reduction with cathodic waves at $E_{1/2} = -0.61$ V with an onset reduction potential (V_{onset}) of −0.52 V versus SCE in CH_3CN solution. The anodic waves were associated with a Re^I-based oxidation process (Re^I/Re^{II}) and the cathodic waves with a ligand-based reduction process ($[Re^ICl(CO)_3(L)]/ [Re^ICl(CO)_3(L^•)]^-$).[17,22] As a result, E_{LUMO} and E_{HOMO} are calculated according to the following

$$E_{LUMO} = -4.74 - V_{onset} \quad (1)$$

$$E_{HOMO} = E_{LUMO} - 1240/\lambda(\text{Abs}) \quad (2)$$

where, −4.74 V is for the SCE with respect to the zero vacuum level;[23] λ(Abs) presents the longest absorption wavelength that can be obtained from the absorption spectrum (Figure 5).

Photophysical Properties. Figure 5 presents the absorption spectrum of Dicnpp-Re in dilute dichloromethane and the PL spectra of Dicnpp-Re, CBP, and CBP/Dicnpp-Re (50%) films. The major absorption bands in 260−360 nm region are assigned to the intraligand ($\pi \rightarrow \pi^*$ (L)) transitions according to the absorption spectrum of the Dicnpp, and a minor absorption band from 360 to 520 nm is tentatively assigned to the metal to ligand charge-transfer $d\pi(Re) \rightarrow \pi^*(N-N)$ (MLCT) transitions. The PL spectrum of CBP with $\lambda_{max} = 380$ nm largely overlaps with the MLCT absorption spectrum of Dicnpp-Re, which demonstrates that Förster energy transfer probably exists during the process of UV or electrical excitation. As the CBP/Dicnpp-Re

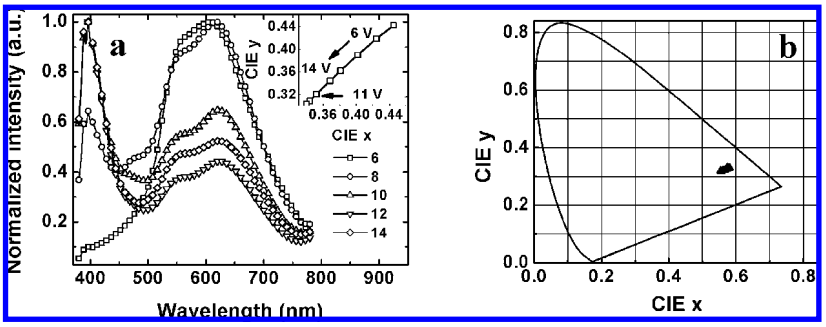

Figure 10. (a) Normalized EL spectra of the devices based on 3% Dicnpp-Re with various applied bias. (b) CIE coordinates of the EL devices based on 16% Dicnpp-Re under different applied bias.

(50%) film is optically excited at $\lambda_{max} = 365$ nm, the ^{3}MLCT emission band centered at 560 nm from the neat Dicnpp-Re film is missing and another new emission band centered at 615 nm appears, which is attributed to the formation of the exciplex between Dicnpp-Re and CBP. Figure 6 presents the formation of the exciplex. The excitation of the molecule of Dicnpp-Re with the lower E_{LUMO} is followed by electron transfer to the other molecule of CBP with the higher E_{HOMO}. The resulting complex electron−hole pair then decays via photon emission with longer wavelength compared to that from either of the individual molecules. As can be seen from Figure 7, the excited-state lifetimes of the neat Dicnpp-Re film (detected at $\lambda_{em} =$ 560 nm) and the CBP/Dicnpp-Re film (detected at $\lambda_{em} = 615$ nm) are 110 and 4 ns, respectively. The shorter lifetime of the blended film, together with the energy diagram of the EL device presented in Figure 2, indicates that the PL spectra centered at 615 nm should originate from the singlet state of the exciplex.

AFM Images. In order to study the film forming behavior of Dicnpp-Re doped CBP films, we show the AFM images of 10% Dicnpp-Re-doped CBP and pure CBP films in Figure 8. The 10% Dicnpp-Re doped CBP film is obviously smoother than the pure CBP film, indicating that the two complexes have good compatibility with each other. At the same time, the surface roughness is calculated to be 0.780 and 7.847 nm for 10% Dicnpp-Re-doped CBP and pure CBP films, respectively, presenting that suitable doping Dicnpp-Re into CBP would lead to the smoother film, which should be beneficial to the EL devices.[24]

EL Properties. Figure 9 shows the current density−luminance−voltage ($J-L-V$) characteristics of the EL device based on 3% Dicnpp-Re, from which white light emission with a CIE coordinate of (0.35, 0.32) is observed under 11 V bias. A maximum brightness of 1457 cd/cm^2 at 14 V and a maximum efficiency of 1.6 cd/A at 5 V are achieved. The relatively lower optimum doping concentration of 3% compared to the traditional electrophosphorescent devices indicates that the Dexter energy transfer mechanism should not be efficient during the EL process. Meanwhile, the E_{HOMO} of Dicnpp-Re is much lower than that of CBP, indicating that the electron-trapping mechanism probably exists. Under applied bias of 13 V, the normalized EL spectra of the devices with different doping concentrations are presented in the inset of Figure 9. When the doping concentration is 3% or below, the EL spectra are composed of mainly three bands: the emission from CBP at ∼390 nm, the ^{3}MLCT emission from Dicnpp-Re at ∼560 nm, and the exciplex emission at ∼620 nm. The former two bands decrease dramatically with the increase of the concentration and almost disappear when the doping concentration is 16%; meanwhile, the exciplex emission band shifts from 620 to 665 nm and finally dominates in the EL spectra. The strong emission from CBP suggests that the considerable recombination region locates in the CBP bulk layer at a lower doping concentration. The E_{HOMO} of Dicnpp-Re is −6.3 eV, which is 0.2 eV lower than that of CBP (Figure 2), indicating that the barrier for hole injection from NPB to CBP would be enhanced with the increase of the doping concentration, so it is reasonable that a faint emission from NPB is observed when the doping concentration is up to 16%.

Figure 10a shows the EL spectra of 3% Dicnpp-Re-based devices with tunable EL emission at various applied bias. Compared with the emission from exciplex or Dicnpp-Re, the CBP-based emission band increases monotonously with the increase of the applied bias from 6 to 14 V, which should be attributed to the higher density of the exciton accumulated in the CBP emission layer at higher applied bias. Correspondingly, the CIE coordinates shift from (0.45, 0.44) to (0.34, 0.30) (Figure 10a inset), indicating that the driving voltage plays an important role in chromaticity tuning. The CIE coordinates of 16% Dicnpp-Re-based EL devices at various applied bias are also presented in Figure 10b. It is found that the EL devices emit pure red light ($x = 0.57$, $y = 0.33$) with only a minor shift of CIE coordinates ($\Delta x = \pm 0.01$, $\Delta y = \pm 0.00$) when the applied bias is changed from 8 to 16 V, implying that Dicnpp-Re holds the greater potential application for color-stable red EL device than the Re(I) complexes reported previously.[3−7]

4. Conclusions

In summary, a Re(I) complex, Dicnpp-Re was synthesized and incorporated in color-tunable EL devices, in which the exciplex emission between Dicnpp-Re and CBP was experimentally realized. The CBP/Dicnpp-Re (3%) based EL device, which emits white light with CIE coordinates of ($x = 0.35$, $y = 0.32$) at 11 V, possesses a maximum brightness of 1457 cd/cm^2 and a peak efficiency of 1.6 cd/A. The longer wavelength emission spectrum (∼615 nm) and the shorter excited-state lifetime (4 ns) for the Dicnpp-Re-doped CBP film confirms the formation of the singlet exciplex between Dicnpp-Re and CBP. The mechanisms of the light-emitting of the OLEDs are also discussed.

Acknowledgment. We gratefully thank the financial support of the One Hundred Talents Project from the Chinese Academy of Sciences and the NSFC (Grant No. 20571071).

Supporting Information Available: X-ray crystallographic data in CIF format of Dicnpp-Re. This material is available free of charge via the Internet at http://pubs.acs.org.

References and Notes

(1) Baldo, M. A.; O' Brien, D. F.; You, Y.; Shoustikov, A.; Sibley, S.; Thompson, M. E.; Forrest, S. R. *Nature* **1998**, *395*, 151.

(2) Bolink, H. J.; Cappelli, L.; Coronado, E.; Grätzel, M.; Ortí, E.; Costa, R. D.; Viruela, P. M.; Nazeeruddin, M. K. *J. Am. Chem. Soc.* **2006**, *128*, 14786.

(3) Li, Y.; Wang, Y.; Zhang, Y.; Wu, Y.; Shen, J. *Synth. Met.* **1999**, *99*, 257.

(4) Wang, K.; Huang, L.; Gao, L.; Jin, L.; Huang, C. *Inorg. Chem.* **2002**, *41*, 3353.

(5) Fu, C.; Li, M.; Su, Z.; Hong, Z.; Li, W.; Li, B. *Appl. Phys. Lett.* **2006**, *88*, 093507.

(6) Li, F.; Zhang, M.; Cheng, G.; Feng, J.; Zhao, Y.; Ma, Y.; Liu, S. *Appl. Phys. Lett.* **2004**, *84*, 148.

(7) Liu, C.; Li, J.; Li, B.; Hong, Z.; Zhao, F.; Liu, S.; Li, W. *Appl. Phys. Lett.* **2006**, *89*, 243511.

(8) Singh, S. P.; Mohapatra, Y. N.; Qureshi, M.; Sundar, M. S. *Appl. Phys. Lett.* **2005**, *86*, 113505.

(9) Palilis, L. C.; Mäkinen, A. J.; Uchida, M.; Kafafi, Z. H. *Appl. Phys. Lett.* **2003**, *82*, 2209.

(10) Liang, C. J.; Choy, W. C. H. *Appl. Phys. Lett.* **2006**, *89*, 251108.

(11) Thompson, J.; Blyth, R. I. R.; Mazzeo, M.; Anni, M.; Gigli, G.; Cingolani, R. *Appl. Phys. Lett.* **2006**, *79*, 560.

(12) Chu, B.; Li, W.; Wei, H.; Wang, D.; Li, M.; Zhang, Z.; Hu, Z.; Lee, C.; Lee, S. *J. Alloys Compd.* **2005**, *389*, 252.

(13) Qureshi, M.; Manoharan, S. S.; Singh, S. P.; Mahapatra, Y. N. *Solid State Commun.* **2005**, *133*, 305.

(14) Hong, Z.; Lengyel, O.; Lee, C.; Lee, S. *Org. Electron.* **2003**, *4*, 149.

(15) Tsuboi, T.; Tanigawa, M.; Kawami, S.; Tsuji, T. *Curr. Appl. Phys.* **2005**, *5*, 47.

(16) Sheldrick, G. M. *SHELXTL*, version 5.10; Siemens Analytical X-ray Instruments Inc.: Madison, WI, 1998. (b) *SMART* and *SAINT*; Siemens Analytical X-ray Instruments Inc.: Madison, WI, 1995. (c) Sheldrick, G. M. *SADABS*; University of Göttingen: Göttingen, Germany, 1996.

(17) Berger, S.; Klein, A.; Kaim, W.; Fiedler, J. *Inorg. Chem.* **1998**, *37*, 5664.

(18) Chen, S.; Xu, X.; Liu, Y.; Yu, G.; Sun, X.; Qiu, W.; Ma, Y.; Zhu, D. *Adv. Funct. Mater.* **2005**, *15*, 1541.

(19) Yam, V. W. W.; Yang, Y.; Zhang, J.; Chu, B.; W. K.; Zhu, N. *Organometallics* **2001**, *20*, 4911.

(20) Zhang, M.; Lu, P.; Wang, X.; He, L.; Xia, H.; Zhang, W.; Yang, B.; Liu, L.; Yang, L.; Yang, M.; Ma, Y.; Feng, J.; Wang, D.; Tamai, N. *J. Phys. Chem. B* **2004**, *108*, 13185.

(21) Rajendran, T.; Manimaran, B.; Lee, F. Y.; Lee, G. H.; Peng, S. M.; Wang, C. C.; Lu, K. L. *Inorg. Chem.* **2000**, *39*, 2016.

(22) Moya, S. A.; Guerrero, J.; Pastene, R.; Schmidt, R.; Sariego, R. *Inorg. Chem.* **1994**, *33*, 2341.

(23) (a) Bard, A. J.; Faulkner, L. R. *Electrochemical Methods: Fundamentals and Applications*; Wiley: New York, 1980. (b) Wu, D. G.; Huang, C. H.; Gan, L. B.; Zheng, J.; Huang, Y. Y.; Zhang, W. *Langmuir* **1999**, *15*, 7276. (c) Ashwini, K. A.; Samson, A. J. *Chem. Mater.* **1996**, *8*, 579.

(24) (a) Zhou, Y.; Sun, Q.; Tan, Z.; Zhong, H.; Yang, C.; Li, Y. *J. Phys. Chem. C* **2007**, *111*, 6862. (b) Xin, Q.; Li, W.; Che, G.; Su, W.; Sun, X.; Chu, B.; Li, B. *Appl. Phys. Lett.* **2006**, *89*, 223524.